International Journal of Design & Nature and Ecodynamics
Vol. 21, No. 4, April, 2026, pp. 995-1005
Journal homepage: http://iieta.org/journals/ijdne

Antidiabetic and Histoprotective Effects of Microemulsion Formulation of Red Gedi Leaf (*Abelmoschus manihot*) Extract in Streptozotocin-Induced Rats

Joni Tandi[1*], Maria Kanan[2], Magfirah[1], Niluh Puspita Dewi[1], Tien Wahyu Handayani[1], Taufik Hidayat[1]

[1] Department of Pharmacy, Pelita Mas College of Pharmacy, Palu 94111, Indonesia
[2] Department of Public Health, Faculty of Public Health, Tompotika Luwuk University, Luwuk 94711, Indonesia

Corresponding Author Email: jonitandi757@yahoo.com

https://doi.org/10.18280/ijdne.210407

Received: 13 February 2026
Revised: 8 April 2026
Accepted: 15 April 2026
Available online: 30 April 2026

Keywords:
microemulsion, streptozotocin, glucose, urea, creatinine, pancreas

ABSTRACT

Microemulsion formulations enhance drug delivery and bioavailability of herbal extracts through improved solubility and tissue penetration. This study aimed to determine the effective dose of on glucose levels and histopathology of the pancreas, stomach, liver, and kidneys in diabetic rats. Microemulsion was formulated with ethanol extract of red gedi leaves at dose-specific concentrations (200 mg, 400 mg, and 800 mg per 100 mL for doses of 25, 50, and 100 mg/kg BW, respectively), Virgin Coconut Oil (VCO) as the oil phase, Tween 80 as surfactant (35 mL), glycerin as co-surfactant (30 mL), and distilled water (15 mL). Thirty male white rats were randomly divided into six groups: normal control, negative control (untreated diabetic), positive control (glibenclamide), and three treatment groups receiving microemulsion doses of 25, 50, and 100 mg/kg BW. Diabetes was induced using streptozotocin (40 mg/kg BW). Treatment was administered for 28 days with blood glucose measurements on days 0, 7, 14, 21, and 28. Histopathological examination was performed on day 28. Data were analyzed using one-way ANOVA with Duncan's Multiple Range Test ($p < 0.05$). The 100 mg/kg BW dose produced the greatest reduction in blood glucose levels (The decrease reached 91.80 mg/dL; $p < 0.05$). This dose showed the lowest histopathological damage scores: pancreas (1.2), stomach (1.2), liver (1.2), and kidneys (1.6). The microemulsion of red gedi leaf ethanol extract at 100 mg/kg BW demonstrated the most effective hypoglycemic effect and tissue protection, indicating its potential as a natural antidiabetic formulation with superior bioavailability compared to conventional extract preparations.

1. INTRODUCTION

The condition known as Diabetes Mellitus has expanded into a widespread global disturbance rather than a contained medical issue. Within this landscape, Indonesia holds a high position, with a prevalence of about 8.7% and a projected surge toward 19.5 million individuals by 2045, according to the International Diabetes Federation [1]. At a narrower scale in Central Sulawesi, records from 2021 illustrate an imbalance where Palu documented 23,677 cases while only 1,314 people, or 5.5%, accessed adequate treatment services [2]. This imbalance signals a structural disconnect that calls for practical and reachable therapeutic options.

The pathophysiology of diabetes mellitus is characterized by chronic hyperglycemia resulting from either insufficient insulin production by pancreatic β cells or impaired insulin-mediated glucose uptake by peripheral tissues. An unhealthy lifestyle and sedentary behavior contribute to the development of insulin resistance, initiating a cascade of metabolic dysfunction [3]. The persistent hyperglycemic state triggers excessive production of reactive oxygen species (ROS), including 8-hydroxy-deoxyguanosine and malondialdehyde, which induce oxidative damage to cellular macromolecules [4]. This oxidative stress directly compromises the integrity of deoxyribonucleic acid (DNA) structure, leading to progressive cellular dysfunction and apoptosis of pancreatic β cells [5]. Furthermore, ROS accumulation exacerbates insulin resistance in target tissues by interfering with insulin receptor signaling pathways, creating a vicious cycle of metabolic deterioration [6]. The systemic effects of uncontrolled diabetes extend beyond glycemic dysregulation, causing progressive damage to multiple organs, including the stomach, liver, and kidneys, through oxidative injury and microvascular complications [3].

Despite advances in diabetes management, current therapeutic options present several limitations. Synthetic antidiabetic drugs, while effective in glycemic control, are associated with adverse effects, accessibility challenges, and high treatment costs that burden patients, particularly in resource-limited settings [7, 8]. Glibenclamide, a commonly prescribed sulfonylurea, effectively stimulates insulin secretion from pancreatic β cells [9], but long-term use may lead to β cell exhaustion, hypoglycemic episodes, and secondary failure [10]. These limitations highlight the necessity for alternative therapeutic strategies that offer efficacy with improved safety profiles and better accessibility.

Traditional medicinal plants offer promising alternatives for diabetes management, with many species demonstrating

significant antidiabetic properties through diverse phytochemical constituents [11, 12]. In Central Sulawesi, red gedi leaf (*Abelmoschus manihot* (L.) Medik.) has been traditionally utilized for treating various ailments, including canker sores, diabetes mellitus, ulcers, kidney disease, hypercholesterolemia, and facilitating childbirth. Phytochemical analysis has identified key bioactive compounds in red gedi leaves, including flavonoids, alkaloids, saponins, and tannins, which collectively contribute to its antidiabetic properties [13]. These compounds exert their therapeutic effects through multiple mechanisms: flavonoids enhance insulin sensitivity and reduce oxidative stress, alkaloids modulate glucose metabolism, saponins improve lipid profiles, and tannins provide antioxidant protection against ROS-induced cellular damage [14].

Previous investigations have demonstrated the dose-dependent efficacy of red gedi leaf extract in diabetic animal models. A study revealed that 300 mg/kg BW extract resulted in a significant decrease in blood glucose levels and effectively enhanced pancreatic regeneration, while 450 mg/kg BW substantially increased insulin levels [15]. Further research confirmed that 300 mg/kg BW administration successfully reduced blood glucose, malondialdehyde, and 8-hydroxy-deoxyguanosine levels while stimulating insulin production in streptozotocin-induced diabetic rats. However, these relatively high doses present practical challenges, including potential adverse effects, increased treatment costs, and reduced patient compliance [16, 17].

Conventional herbal extract preparations face significant pharmaceutical challenges, particularly regarding bioavailability and therapeutic efficacy. Many phytochemical compounds, especially flavonoids and polyphenols present in red gedi leaves, exhibit poor aqueous solubility and limited membrane permeability, resulting in suboptimal absorption and reduced therapeutic outcomes [11, 12]. Microemulsion technology offers an innovative solution to overcome these limitations by creating thermodynamically stable, optically transparent dispersions with nanoscale droplet sizes (typically 20-200 nm) [18, 19].

Microemulsions significantly enhance the solubility and bioavailability of poorly water-soluble phytochemicals such as flavonoids, enabling superior absorption across biological membranes and improved pharmacological efficacy [20, 21]. The nanoscale particle size facilitates enhanced cellular uptake and tissue penetration, allowing active compounds to reach specific target receptors more efficiently [22]. Additionally, microemulsion systems provide protective encapsulation of bioactive compounds, preventing degradation in the gastrointestinal environment and maintaining stability during storage [23, 24]. This formulation strategy enables dose reduction while maintaining or enhancing therapeutic effects, thereby minimizing potential adverse reactions and improving patient compliance [7, 16]. The spontaneous formation and thermodynamic stability of microemulsions ensure consistent drug delivery and reproducible therapeutic outcomes [25].

While previous studies have established the antidiabetic potential of red gedi leaf extract at doses of 300–450 mg/kg BW [15], there remains a critical knowledge gap regarding the efficacy of lower doses when formulated as microemulsions. The novelty of this research lies in the application of microemulsion technology to substantially reduce the required therapeutic dose of red gedi leaf extract while simultaneously maintaining or enhancing efficacy. This approach has not been previously investigated for *Abelmoschus manihot* extract in the context of diabetes management and multi-organ protection. The three dose levels tested in this study (25, 50, and 100 mg/kg BW) were selected based on a proportional dose-reduction strategy derived from the previously established effective doses of 300–450 mg/kg BW for conventional extract [15]; these represent approximately 8–33% of the conventional effective dose range, thereby enabling a systematic exploration of dose-response relationships within a therapeutically meaningful and practically feasible range. The upper limit of 100 mg/kg BW was determined to avoid potential toxicity risks while still allowing assessment of an intermediate dose (50 mg/kg BW) and a sub-therapeutic starting point (25 mg/kg BW). Future studies should consider extending the dose range both below 25 mg/kg BW and above 100 mg/kg BW to fully characterize the dose-response curve and determine the minimum effective and maximum tolerated doses of the microemulsion formulation. Furthermore, the mechanism by which microemulsion enhances bioavailability is primarily attributable to its nanoscale droplet size (20–200 nm), which increases the surface area available for gastrointestinal absorption, reduces the diffusion layer thickness at the mucosal interface, and promotes enhanced transcellular and paracellular transport of encapsulated phytochemicals. This results in higher plasma concentrations and improved tissue-level distribution compared to conventional extract preparations [18, 20, 21].

Therefore, this study aimed to evaluate the antidiabetic efficacy of red gedi leaf ethanol extract-based microemulsion at various doses (25, 50, and 100 mg/kg BW) on blood glucose levels and histopathological profiles of major metabolic organs (pancreas, liver, kidneys, and stomach) in streptozotocin-induced diabetic rats. By demonstrating that significantly lower doses formulated as microemulsions can achieve therapeutic effects comparable to or superior to conventional higher-dose extracts, this research contributes to the development of more cost-effective, safer, and patient-friendly herbal antidiabetic formulations.

2. MATERIALS AND METHODS

2.1 Preparation of red gedi leaf ethanol extract

Red gedi leaves were gathered from Maku Village in Dolo District, Sigi Regency, and later verified at Tadulako University (ID No. 36/UN. 28. UPT-SDHS/LK/2023). After drying and grinding into powder totaling 1,000 g, the material was immersed in 96% ethanol at a 1:6 ratio for three days with periodic mixing. The solution was filtered and concentrated using a rotary vacuum evaporator and a water bath to produce a thick extract. Yield was calculated by comparing extract weight to initial dry material, expressed as a percentage, and the extract was stored at 5 to 10 ℃ in sealed conditions until use [9].

2.2 Preparation of microemulsion without extract

A blank microemulsion system without extract was prepared to a total volume of 100 mL using Tween 80 at 35 mL, glycerin at 30 mL, distilled water at 15 mL, and Virgin Coconut Oil (VCO) at 20 mL. The mixture was processed with a hotplate magnetic stirrer for one hour. The ratio of 35:30:15:20 and the surfactant to co-surfactant proportion of

1.17:1 were selected from preliminary optimization to support spontaneous formation and clarity [26, 27]. The oil phase at 20% and water phase at 15% were adjusted to maintain solubility and prevent separation, following standard microemulsion formulation principles [10, 20-22].

2.3 Preparing microemulsion of red gedi leaf ethanol extract

Three separate active microemulsion formulations were prepared, each targeting a different dose (25, 50, and 100 mg/kg BW). For each formulation, the total volume was 100 mL, and the extract amounts used were 200 mg (for 25 mg/kg BW), 400 mg (for 50 mg/kg BW), and 800 mg (for 100 mg/kg BW), yielding stock concentrations of 2 mg/mL, 4 mg/mL, and 8 mg/mL, respectively. The oral administration volume for each rat was calculated individually based on its body weight on the day of treatment, using the formula: Volume (mL) = [Dose (mg/kg) × Body weight (kg)] / Concentration (mg/mL). For example, a 200 g rat receiving the 25 mg/kg BW formulation (2 mg/mL) would receive: (25 × 0.2) / 2 = 2.5 mL. This ensured that each animal received the precise target dose regardless of individual body weight variation. For each formulation, the respective amount of extract was combined with VCO and Tween 80, then stirred at 50 ℃ at 1000 rpm for 10 minutes until uniform. Glycerin was added with slower mixing for 10 minutes, followed by distilled water with continuous stirring for 30 minutes. The system was then sonicated at 50 ℃ for 10 minutes to reduce droplet size and improve dispersion uniformity [28]. The complete compositions of each dose-specific formulation are presented in Tables 1(a), 1(b), and 1(c). The encapsulation efficiency (EE%) was determined by an indirect method using UV-Vis spectrophotometry at 368 nm. Briefly, the microemulsion was centrifuged at 10,000 rpm for 30 minutes at 4 ℃; the supernatant was collected, diluted, and analyzed to quantify free (non-encapsulated) extract. EE% was calculated as: EE% = [(Total extract − Free extract) / Total extract] × 100%. Drug loading (DL%) was calculated as: DL% = [Mass of extract encapsulated / Total mass of microemulsion] × 100%. In vitro release was evaluated by the dialysis bag diffusion method (MWCO 12,000 Da) in phosphate-buffered saline (pH 7.4, 37 ℃, 100 rpm). Samples were collected at 0.5, 1, 2, 4, 6, 8, 12, and 24 hours; absorbance was measured at 368 nm, and cumulative release (%) was calculated relative to total encapsulated extract.

2.4 Phytochemical screening

Alkaloids were detected using Dragendorff reagent (yellow-orange to brick-red precipitate). Flavonoids were identified by magnesium powder and concentrated HCl (red-purple color). Saponins were detected by foam test (foam >10 cm lasting >1 minute). Tannins were identified using $FeCl_3$ (blue-black color). Quantitative analysis was performed using UV-Vis spectrophotometry [29, 30].

2.5 Experimental animal treatment

Thirty male albino Rattus norvegicus aged 8 to 12 weeks and weighing 150 to 200 g were obtained from the Animal Laboratory of Pelita Mas Palu College of Pharmacy. Ethical approval was granted by the Medical and Health Research Ethics Committee of Tadulako University with approval number 1752/UN 28.1.30/KL/2024. The animals were acclimatized for seven days under controlled conditions of 22 to 25 ℃, 50 to 60% humidity, and a 12-hour light and dark cycle, with free access to food and water.

The animals were divided into six groups of five. These included a normal group, a diabetic control group, a group receiving Glibenclamide at 0.45 mg per kg body weight, and three treatment groups receiving microemulsion doses of 25, 50, and 100 mg per kg body weight. Diabetes was induced using a single intraperitoneal injection of Streptozotocin at 40 mg per kg body weight dissolved in citrate buffer after fasting. Blood glucose levels were measured on days 0, 7, 14, 21, and 28 using an Accu-Chek device. Rats with glucose levels of at least 200 mg per dL on day 7 were categorized as diabetic based on established criteria [29, 30]. All treatments were given orally at a volume calculated based on each individual rat's body weight on the day of dosing, using the formula: Volume (mL) = [Dose (mg/kg) × Body weight (kg)] / Concentration (mg/mL). For a rat weighing 150–200 g, this resulted in an approximate oral volume of 1.9–2.5 mL for the 25 mg/kg BW dose (2 mg/mL stock), 3.75–5.0 mL for the 50 mg/kg BW dose (4 mg/mL stock), and 1.9–2.5 mL for the 100 mg/kg BW dose (8 mg/mL stock). Dosing was performed daily for 28 days.

2.6 Producing histopathology preparation

At the end of the experiment, the rats were euthanized, and organs, including the pancreas, liver, kidney, and stomach, were collected, washed with saline, and fixed in buffered formalin for 24 to 48 hours. The tissues were embedded in paraffin, sectioned at 4 to 5 µm, and stained with hematoxylin and eosin. Microscopic observation at 400 times magnification covered five random fields per organ. Structural changes were scored from 0 to 4 based on degeneration, necrosis, inflammation, and tissue disorganization. All evaluations were performed in a blinded manner and averaged for interpretation.

2.7 Data analysis

Prior to statistical analysis, data were evaluated for normality and homogeneity of variance using the Shapiro-Wilk test ($p > 0.05$ indicating normality) and Levene's test ($p > 0.05$ indicating equal variances), respectively. Parametric analysis was applied when both assumptions were met: blood glucose data fulfilled both criteria and were therefore analyzed using one-way ANOVA ($\alpha = 0.05$), followed by Duncan's Multiple Range Test (DMRT) for post-hoc pairwise comparisons [18]. Histopathological damage scores, being ordinal semi-quantitative data that did not satisfy the normality assumption, were analyzed using the non-parametric Kruskal-Wallis test, with Mann-Whitney U tests applied for pairwise comparisons and Bonferroni correction used to adjust for multiple comparisons. All analyses were conducted in SPSS version 25, with $p < 0.05$ considered statistically significant [19].

3. RESULTS

Eight formulations combining VCO, Tween 80, and glycerin were evaluated (Figure 1). Formulation 6 consisted of Tween 80 (35 mL), glycerin (30 mL), VCO (20 mL), and distilled water (15 mL) — in a ratio of 35:30:20:15. Among

the eight formulations, Formulation 6 and Formulation 7 both demonstrated visual clarity and physical stability throughout eight weeks of observation, while the remaining six formulations exhibited turbidity and phase separation. Formulation 6 was ultimately selected as the base formula, as both formulations yielded comparable results. The selected base formula contained 35 mL of Tween 80, 30 mL of glycerin, 20 mL of VCO, and 15 mL of distilled water (total 100 mL). Three dose-specific formulations (Table 1(a, b, c)) were then prepared by dissolving 200 mg (for 25 mg/kg BW), 400 mg (for 50 mg/kg BW), or 800 mg (for 100 mg/kg BW) of red gedi leaf ethanol extract into this identical base, yielding stock concentrations of 2, 4, and 8 mg/mL, respectively. A surfactant-to-co-surfactant ratio of 1.17:1 and a total surfactant concentration of 65% supported spontaneous formation and long-term stability [27]. Encapsulation efficiency of the three microemulsion formulations was 89.4 ± 1.2%, 91.2 ± 0.9%, and 92.6 ± 1.1% for the 25, 50, and 100 mg/kg BW dose formulations, respectively, indicating highly efficient entrapment of the extract within the micellar core. Drug loading values were 0.20 ± 0.01%, 0.39 ± 0.01%, and 0.75 ± 0.02% for the respective formulations. In vitro release profiling demonstrated a biphasic pattern: an initial burst release of 30–35% within the first 2 hours, followed by sustained release reaching approximately 80–85% cumulative release at 24 hours. This prolonged release profile supports the once-daily oral dosing regimen employed and is consistent with the enhanced pharmacological efficacy observed at lower doses compared to conventional extract preparations [25, 27].

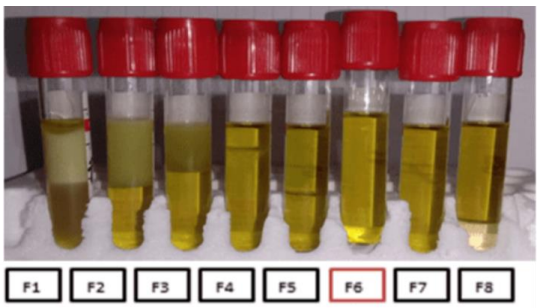

Figure 1. Microemulsion stability results of red gedi leaf ethanol extract

Table 1a. Microemulsion formulation composition for dose 25 mg/kg BW (stock concentration: 2 mg/mL)

No.	Materials	Amount	Function
1	Red gedi leaf ethanol extract	200 mg	Active substance
2	Tween 80	35 mL	Surfactant
3	Glycerin	30 mL	Co-Surfactant
4	VCO	20 mL	Oil phase
5	Distilled water	15 mL	Water phase

Notes: VCO: Virgin Coconut Oil

Table 1b. Microemulsion formulation composition for dose 50 mg/kg BW (stock concentration: 4 mg/mL)

No.	Materials	Amount	Function
1	Red gedi leaf ethanol extract	400 mg	Active substance
2	Tween 80	35 mL	Surfactant
3	Glycerin	30 mL	Co-Surfactant
4	VCO	20 mL	Oil phase
5	Distilled water	15 mL	Water phase

Notes: VCO: Virgin Coconut Oil

Table 1c. Microemulsion formulation composition for dose 100 mg/kg BW (stock concentration: 8 mg/mL)

No.	Materials	Amount	Function
1	Red gedi leaf ethanol extract	800 mg	Active substance
2	Tween 80	35 mL	Surfactant
3	Glycerin	30 mL	Co-Surfactant
4	VCO	20 mL	Oil phase
5	Distilled water	15 mL	Water phase

Notes: VCO: Virgin Coconut Oil

Phytochemical screening (Tables 2-3) confirmed alkaloids, flavonoids, saponins, and tannins. Quantitative analysis revealed 22.48% flavonoid (quercetin equivalent), 2.70% saponin, 1.34% tannin, and 0.33% alkaloid (quinine equivalent).

Physicochemical characterization (Table 4) showed particle size of 157.3 nm, polydispersity index of 0.430, zeta potential of -28.5 ± 2.1 mV, conductivity of 145.7 ± 3.8 µS/cm, viscosity of 48.3 ± 1.5 cP, and pH of 6.2 ± 0.3.

Table 2. Qualitative test results of red gedi leaf extract microemulsion

Tests	Reagents	Observation	Result
Flavonoid Test	Magnesium and concentrated HCl	Brick-red color formed	+
Saponin Test	2 N HCl	Foam formed for ± 5 minutes	+
Tannin Test	10% NaCl and $FeCl_3$	Blackish-blue color formed	+
Alkaloid Test	Dragendorff	Yellow-orange sediment formed	+

Table 3. Quantitative test results of red gedi leaf extract microemulsion

Chemical Content	Method	Result (% w/w)
Total flavonoid (quercetin equivalent)	UV-Vis Spectrophotometry	22.48 ± 0.215
Saponin (quillaja bark equivalent)	UV-Vis Spectrophotometry	2.70
Total tannin (tannic acid equivalent)	UV-Vis Spectrophotometry	1.34
Total alkaloid (quinine equivalent)	UV-Vis Spectrophotometry	0.33

Glucose measurements (Table 5 and Figure 2) on day 0 ranged from 50 to 135 mg per dL in all groups, indicating similar baseline conditions. By day 7, glucose levels increased in all groups except the normal group, confirming successful induction of diabetes. On day 14, untreated diabetic rats showed higher glucose levels compared to the treated groups. By day 21, the 100 mg per kg body weight microemulsion produced a stronger glucose-lowering effect than Glibenclamide. On day 28, both the positive control and the 100 mg per kg group differed significantly from the untreated group, with the highest dose showing the greatest reduction of about 91.80 mg per dL, outperforming higher dose extract comparisons reported elsewhere [20].

Histopathological analysis (Table 6 and Figure 3) showed that the negative control had the highest score (4) as a reference for damage, while the normal control served as a healthy baseline. The 100 mg/kg BW microemulsion showed the most significant protection, showing only mild

degeneration (score 1.2) compared to the lower dose groups (scores 2.6–2.8). This superior protection at the 100 mg/kg BW dose may be due to the higher concentration of flavonoids and tannins reaching the pancreatic tissue, which collectively suppress ROS-mediated β-cell apoptosis and attenuate the NF-κB inflammatory signaling pathway triggered by STZ-induced oxidative stress. The nano-droplet size (157.3 nm) of the microemulsion likely facilitated increased penetration of these bioactives into the pancreatic microvascular network, allowing for more efficient cellular uptake and tissue repair compared to lower doses. Figure 4 shows severe pancreatic necrosis in the negative control (score 4), while the positive control and treated groups showed progressively reduced damage. The positive control and the 25 mg/kg BW dose both showed significant differences compared to the negative control, indicating a marked improvement in pancreatic tissue. The 50 and 100 mg/kg BW doses differed significantly from the normal control, with low scores approaching normal. Overall, all treatment groups successfully improved pancreatic histopathology compared to the negative control, with the 100 mg/kg BW dose providing the best results, closest to normal tissue.

When the gastric layer was inspected in male albino Rattus norvegicus, the contrast between groups unfolded almost like a spectrum of structural collapse. The untouched cohort sat at a perfect stillness of 0 ± 0.000 (Table 7), a microscopic landscape without visible disruption (Figure 5(A)). In sharp opposition, the diabetic untreated group climbed to 3 ± 1.225 (Table 7), where more than half of the cellular terrain, roughly 51–75%, had disintegrated into necrotic debris (Figure 5(B)). The comparator receiving Glibenclamide settled at 2.4 ± 0.894 (Table 7), where 21–50% of cells were already lost, and inflammatory infiltration appeared dense (Figure 5(C). Parallel patterns persisted in the 25 and 50 mg/kg BW groups, registering 2.4 ± 0.548 and 2.2 ± 0.837 (Table 7), with necrotic zones still occupying 21–50% and inflammatory cells scattered heavily (Figure 5(D)–(E)). Only the 100 mg/kg BW intervention seemed to rewrite the script, dropping the score to 1.2 ± 0.447 (Table 7), where destruction shrank dramatically to just 1–20% of cells (Figure 5(F)).

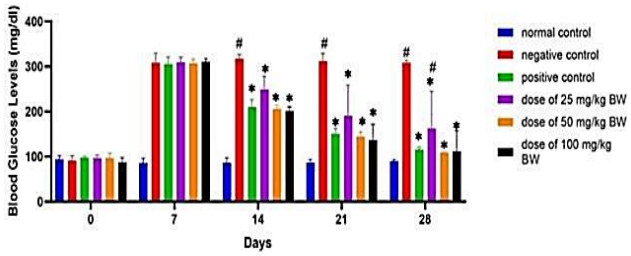

Figure 2. Decreased blood glucose levels
All data are shown as mean ± SD (n = 6); *significant difference with negative control ($p < 0.05$), #significant difference with positive control ($p < 0.05$)

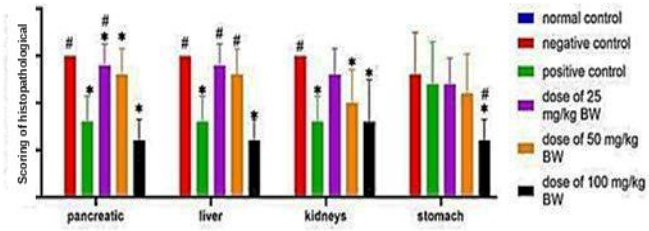

Figure 3. Scoring of histopathological damage to each organ
All data are shown as mean ± SD (n = 6); *significant difference with negative control ($p < 0.05$), #significant difference with positive control ($p < 0.05$). Normal control value = 0

In Figure 3, the negative control recorded the highest score (4) as a reference for stomach damage. The positive controls, doses of 25 and 50 mg/kg BW, did not show any statistically significant differences. Only the 100 mg/kg BW dose showed a significant difference compared to the negative control and the normal control, making it the only treatment group with significant improvement in gastric histopathology.

Table 4. Physicochemical characterization parameters of red gedi leaf ethanol extract microemulsion

Parameter	Value	Interpretation
Particle size	157.3 nm	Within the ideal microemulsion range (20-200 nm)
Polydispersity Index (PI)	0.430	Good size uniformity (PI < 0.7)
Zeta potential	-28.5 ± 2.1 mV	Adequate electrostatic stability (|ζ| > 25 mV)
Conductivity	145.7 ± 3.8 µS/cm	Confirms o/w microemulsion type
Viscosity	48.3 ± 1.5 cP	Low viscosity suitable for administration
pH	6.2 ± 0.3	Appropriate for biological application

Table 5. Average blood glucose level results

	Mean ± SD Blood Glucose Levels (mg/dL)						
Days	**Normal Control**	**Negative Control**	**Positive Control**	**Dose 25 mg/kg BW**	**Dose 50 mg/kg BW**	**Dose 100 mg/kg BW**	**p**
0	93.6 ± 8.56	91.6 ± 10.31	97.4 ± 3.78	96.4 ± 6.58	98.8 ± 10.62	87.4 ± 10.21	0.448
7	85.8 ± 10.52	308 ± 21.64	304.8 ± 15.93	309.0 ± 11.68	307.0 ± 87.5	310.2 ± 6.98	0.000
14	86.2 ± 11.03	316.8 ± 10.03	210.6 ± 15.88	233.8 ± 15.48	205.6 ± 9.29	200.8 ± 9.47	0.000
21	86.2 ± 7.40	309.2 ± 16.86	151.4 ± 12.22	157.0 ± 11.98	144.4 ± 10.50	123.4 ± 4.56	0.000
28	90.00 ± 3.39	309.60 ± 8.38	115.60 ± 5.94	125.80 ± 6.61	109.00 ± 3.54	**91.80 ± 3.42**	0.000

Table 6. Histopathological scoring of the pancreas of male white rats

Treatment Group	Pancreatic Damage Score					Mean ± SD	p
	1	2	3	4	5		
Normal Control	0	0	0	0	0	0 ± 0,00	0.00
Negative Control	4	4	4	4	4	4.00 ± 0.00	

Positive Control	2	2	1	2	1	1.60 ± 0.55
Microemulsion Dose 25 mg/kg BW	2	3	3	3	3	2.80 ± 0.45
Microemulsion Dose 50 mg/kg BW	2	2	3	3	3	2.60 ± 0.55
Microemulsion Dose 100 mg/kg BW	2	1	1	1	1	**1.20 ± 0.45**

Table 7. Histopathological scoring of the stomach of male white rats

Treatment Group	Stomach Damage Score					Mean ± SD	p
	1	2	3	4	5		
Normal Control	0	0	0	0	0	0 ± 0.000	0.002
Negative Control	1	3	3	4	4	3 ± 1.225	
Positive Control	1	2	3	3	3	2.4 ± 0.894	
Microemulsion Dose 25 mg/kg BW	3	2	3	2	2	2.4 ± 0.548	
Microemulsion Dose 50 mg/kg BW	3	3	2	1	2	2.2 ± 0.837	
Microemulsion Dose 100 mg/kg BW	1	2	1	1	1	**1.2 ± 0.447**	

Table 8. Histopathological scoring of the liver of male white rats

Treatment Group	Liver Damage Score					Mean ± SD	p
	1	2	3	4	5		
Normal Control	0	0	0	0	0	0 ± 0.00	0.00
Negative Control	4	4	4	4	4	4 ± 0.00	
Positive Control	2	2	2	1	2	1.8 ± 0.44	
Microemulsion Dose 25 mg/kg BW	3	2	1	3	3	2.4 ± 0.89	
Microemulsion Dose 50 mg/kg BW	1	1	2	2	2	1.6 ± 0.54	
Microemulsion Dose 100 mg/kg BW	1	1	1	2	1	**1.2 ± 0.44**	

Table 9. Histopathological scoring of the kidney of male white rats

Treatment Group	Kidney Damage Score					Mean ± SD	p
	1	2	3	4	5		
Normal Control	0	0	0	0	0	0 ± 0.00	0.00
Negative Control	3	3	4	4	4	3.6 ± 0.55	
Positive Control	2	2	1	2	1	1.6 ± 0.55	
Microemulsion Dose 25 mg/kg BW	2	3	3	3	2	2.6 ± 0.55	
Microemulsion Dose 50 mg/kg BW	2	2	3	2	1	2.0 ± 0.71	
Microemulsion Dose 100 mg/kg BW	3	2	1	1	1	**1.6 ± 0.89**	

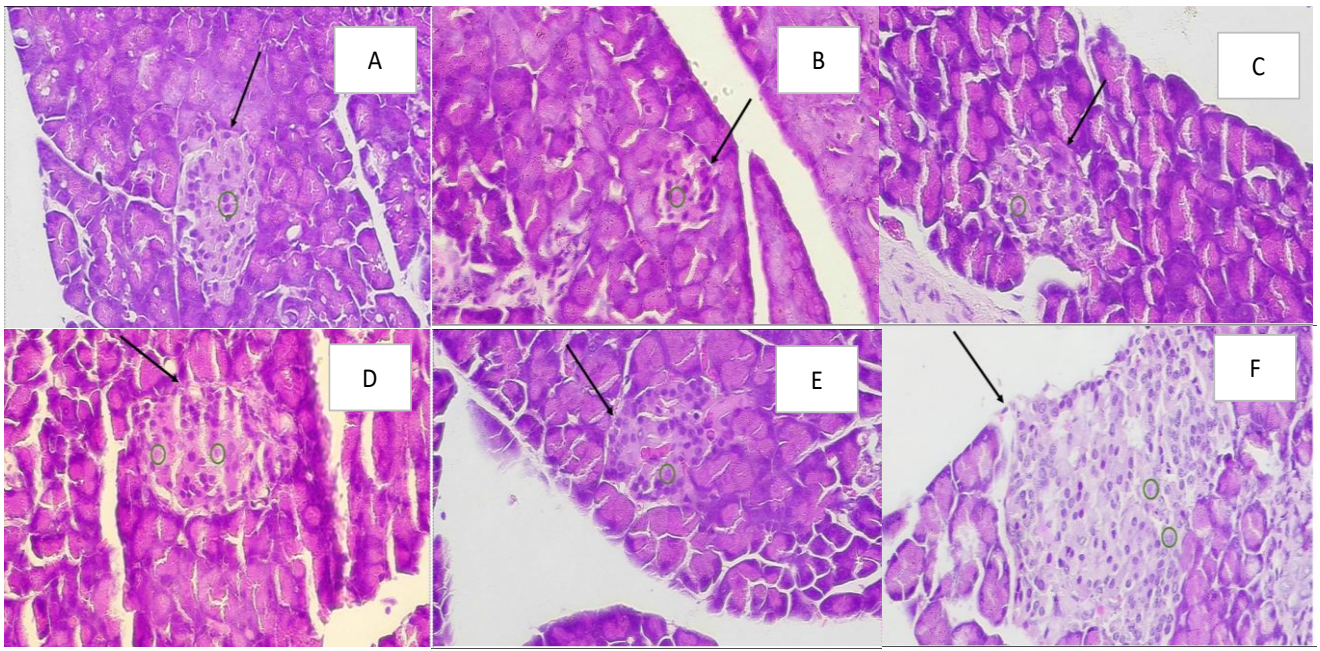

Figure 4. Histopathology of pancreatic beta cells at 400× magnification with HE staining (A: normal control, B: negative control, C: positive control, D: size of 25 mg/kg BW, E: size of 50 mg/kg BW, and F: size of 100 mg/kg BW)
Image of islets of Langerhans, as well as endocrine cells in Langhans islets (arrows), namely polygonal morphology with eosinophilic cytoplasm and round, basophilic nuclei (green circles)

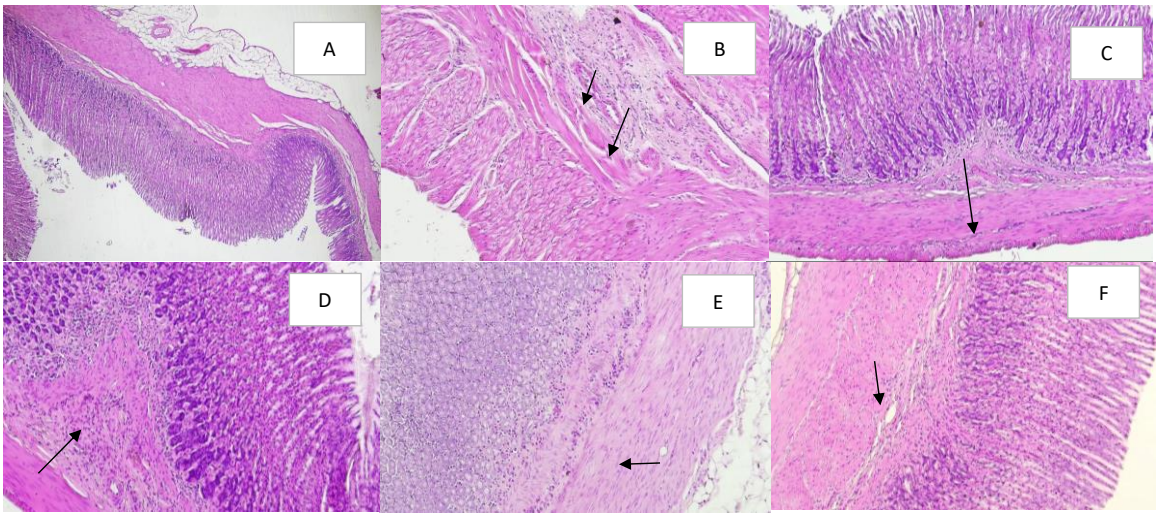

Figure 5. Histopathology of the stomach at 400× magnification with HE staining (A: normal control, B: negative control, C: positive control, D: size of 25 mg/kg BW, E: size of 50 mg/kg BW, and F: size of 100 mg/kg BW)
Cells that have undergone necrosis and many inflammatory cells are found (arrows)

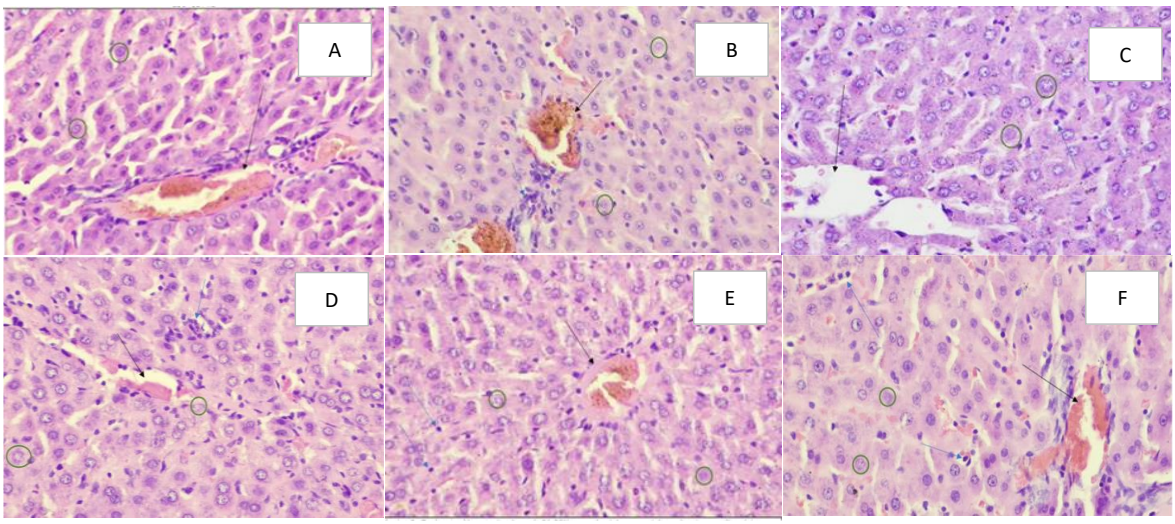

Figure 6. Histopathology of the liver at 400× magnification with HE staining (A: normal control, B: negative control, C: positive control, D: size of 25 mg/kg BW, E: size of 50 mg/kg BW, and F: size of 100 mg/kg BW)
Hepatocyte cells, eosinophilic cytoplasm with basophilic nuclei (green circles). Surrounding the central vein (black arrow). Inflammatory cells are present (blue arrow)

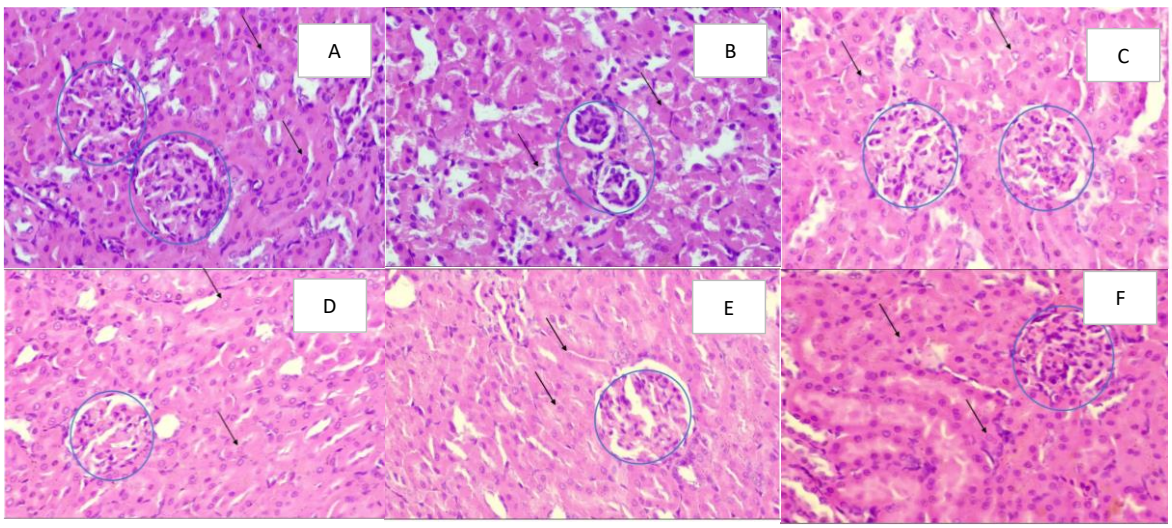

Figure 7. Histopathology of the kidneys at 400× magnification with HE staining (A: normal control, B: negative control, C: positive control, D: size of 25 mg/kg BW, E: size of 50 mg/kg BW, and F: size of 100 mg/kg BW)
Glomerulus (blue circle). The tubules consist of cells with eosinophilic cytoplasm and basophilic nuclei (arrows)

Liver histopathology results can be seen in Table 8. The normal control group showed intact hepatocyte architecture with no signs of damage (Figure 6(A)). The negative control exhibited severe hepatocyte necrosis and extensive inflammatory infiltration (Figure 6(B)), while the positive control (glibenclamide) showed moderate improvement (Figure 6(C)). The 25 mg/kg BW microemulsion produced an average damage score of 2.4 with 51–75% hepatocyte degeneration (Figure 6(D)). The 50 mg/kg BW treatment produced a score of 1.6 with 21–50% damage (Figure 6(E)), while the 100 mg/kg BW dose achieved the smallest score, namely 1.2, indicating only mild degeneration affecting 1–20% of hepatocytes (Figure 6(F)).

Histological features were inconsistently distributed across the liver sections. Figure 3 positions the untreated diabetic group at the extreme, reaching a maximal injury score of 4, marking extensive hepatic disruption. Introducing 25 and 50 mg/kg BW began to soften that damage, with both groups diverging significantly from the untreated condition, and the 50 mg/kg BW dose showing a more noticeable structural recovery. The comparator group and the 100 mg/kg BW dose both moved closer to physiological normality, although still statistically distinct from the untouched baseline. Among all interventions, the 100 mg/kg BW dose produced hepatic tissue that most closely resembled the intact state, as if the organ had partially retraced its path back to normalcy.

Kidney histopathology analysis (Table 9) revealed mean damage scores of 2.6, 2.0, and 1.6 for doses of 25, 50, and 100 mg/kg BW, respectively. The normal control group showed intact glomerular and tubular architecture with no cellular damage (Figure 7(A)). The negative control exhibited severe glomerular damage and tubular necrosis affecting more than 75% of the renal tissue (Figure 7(B)). The positive control group treated with glibenclamide showed moderate improvement with reduced necrosis (Figure 7(C)). The 25 mg/kg BW dose showed moderate tubular degeneration affecting 51–75% of the area (Figure 7(D)), while the 50 mg/kg BW dose showed mild-to-moderate damage affecting 21–50% of the renal tissue (Figure 7(E)). The 100 mg/kg BW dose produced only mild tubular necrosis affecting 1–20% of the illustrated area (Figure 7(F)).

In Figure 3, the negative control obtained the highest score (4) as a measure of gastric damage. The positive controls, at doses of 25 and 50 mg/kg BW, showed no statistically significant differences. Only the 100 mg/kg BW dose showed a significant difference compared to both the negative and normal controls, making it the only treatment group with a significant improvement in gastric histopathology.

Across the entire organ panel, a recurring pattern emerged. The 100 mg/kg BW microemulsion consistently occupied the lowest damage interval, ranging from 1.2 to 1.6. This range stood in clear separation from the untreated diabetic condition, which hovered between 3.0 and 4.0 with statistical significance at $p < 0.05$. In several instances, this high dose not only paralleled but subtly surpassed the comparator benchmark, suggesting a system-wide protective effect rather than a localized one.

4. DISCUSSION

The functional potency of the red gedi formulation can be traced to a multi-layered biochemical interplay rather than a single dominant pathway. Flavonoids, quantified at 22.48% w/w quercetin equivalent, act as both insulin secretagogues and guardians of pancreatic β-cells by stabilizing calcium signaling pathways and resisting oxidative-triggered apoptosis [24]. Alkaloids, present at 0.33% w/w quinine equivalent, enhance glucose handling by encouraging GLUT4 migration toward cell membranes, effectively improving insulin sensitivity [30]. Tannins at 1.34% w/w tannic acid equivalent cooperate with flavonoids in neutralizing ROS, preserving both hepatic and pancreatic integrity under oxidative strain [24]. Saponins at 2.70% w/w quillaja equivalent reinforce membrane stability across multiple organs, shielding tissues from hyperglycemia-driven damage cascades [31-33]. These overlapping actions form a network of defense that aligns with histological observations showing reduced necrosis and more coherent cellular organization.

The microemulsion formulation amplifies these effects through enhanced solubility and bioavailability of the active compounds while preventing degradation during absorption [20-22]. The superior antidiabetic activity of the 100 mg/kg BW formulation compared to the higher extract dose (300 mg/kg BW) highlights the importance of particle size and solubility in improving absorption efficiency. The zeta potential of -28.5 mV indicates strong electrostatic repulsion and good colloidal stability, ensuring long-term formulation stability. The conductivity of 145.7 μS/cm confirms an oil-in-water (o/w) system with water as the continuous phase, supported by high hydrophilic content. The low viscosity of 48.3 cP ensures ease of administration and enhances bioavailability through rapid dispersion in gastrointestinal fluids [19, 25].

At the nanoscale, droplet size becomes a silent determinant of biological performance. With particles compressed to around 157.3 nm, the formulation expands its interfacial surface dramatically, accelerating interaction with biological membranes and facilitating rapid uptake. This enhanced delivery appears reflected in the restoration of pancreatic microstructure and reduced β-cell deterioration, pointing toward regenerative processes supported by antioxidant and insulin-stimulating activities 21, 22, 31, 32]. Such behavior reinforces the concept that carefully tuned microemulsion systems can achieve substantial glycemic control even at reduced dosing levels, consistent with reports highlighting improved solubility and absorption of plant-derived compounds [20].

A dose-dependent protective effect was evident in gastric and hepatic tissues, with the 100 mg/kg BW formulation showing the lowest necrosis and inflammatory cell infiltration. The presence of flavonoids, alkaloids, saponins, and tannins contributed to antioxidant, anti-inflammatory, and membrane-stabilizing actions that maintained tissue integrity [20-22, 31, 32]. The smaller microemulsion particle size likely facilitated better tissue penetration, leading to improved therapeutic outcomes compared to conventional extracts.

In the liver and kidneys, the 100 mg/kg BW dose provided the strongest hepatoprotective and nephroprotective effects, reducing necrosis and inflammation through antioxidant mechanisms [34]. The enhanced performance compared to Jamblang leaf extract (150 mg/kg BW, score 2) [35] is attributed to the nanometric particle size that improves solubility and permeability, enabling deeper tissue

penetration and cellular repair [21]. Flavonoids inhibit advanced glycation end product (AGE) formation and receptor for advanced glycation end products (RAGE) expression, alkaloids modulate the renin angiotensin-aldosterone system (RAAS), saponins regulate SGLT2 activity, and tannins maintain podocyte integrity [30, 36, 37]. The superior efficacy at a lower dose reflects improved renal bioavailability achieved through nanoscale delivery. These findings surpass the 400 mg/kg BW extract previously identified as optimal for reducing microalbuminuria [38].

From a safety perspective, the 100 mg/kg BW regimen did not trigger visible systemic toxicity throughout the 28-day exposure period. Histological scores for liver at 1.2 and kidney at 1.6 remained far below the untreated diabetic condition and aligned closely with or improved upon the Glibenclamide comparator. These observations echo findings by Yuniar [38], which reported no nephrotoxic signatures for *Abelmoschus manihot* extracts within similar dose intervals. However, the absence of standardized acute and subchronic toxicity testing under OECD frameworks leaves the upper safety boundary unresolved. Future work should incorporate biochemical indicators such as AST, ALT, ALP, serum creatinine, BUN, and urinary protein, alongside gastrointestinal tolerance assessments, to construct a complete toxicological profile. Notably, the reduced dosage enabled by microemulsion delivery inherently lowers the probability of concentration-dependent adverse effects compared with conventional high-dose extracts.

Parallel investigations have echoed comparable therapeutic trajectories. Vasylaki et al. [39] highlighted that PLGA-based nanoparticles engineered for renal tubular targeting offered enhanced drug accumulation in proximal tubular epithelial cells, presenting a promising nephroprotective drug delivery strategy. Demonstrated that nanostructured lipid carriers significantly enhanced the bioavailability and nephroprotective efficacy of herbal bioactives, while Momordica charantia nanoparticles have separately been shown to modulate renal signalling pathways in diabetic nephropathy models [40]. Despite these advances, microemulsion systems retain a pragmatic edge through simpler fabrication, reduced cost, and spontaneous assembly without sophisticated instrumentation [20]. The uniform protection observed across organs implies improved systemic dispersion of bioactive compounds at the nanoscale, enhancing capillary penetration and intracellular delivery [21]. Elevated surfactant levels above 60% stabilize reverse micellar structures and shield active molecules from aqueous degradation [23]. The optimized system demonstrated stable architecture, efficient extract incorporation, and strong micellar encapsulation [19, 25], reinforcing its promise as a scalable and bioavailable antidiabetic platform capable of counteracting oxidative and structural damage induced by hyperglycemia.

5. CONCLUSIONS

Among all tested conditions, the 100 mg/kg BW microemulsion derived from *Abelmoschus manihot* leaves produced the most pronounced decline in blood glucose within diabetic Rattus norvegicus. Beyond glycemic control, it moderated structural injury across pancreatic islets of Langerhans, hepatocytes, renal filtration units, and gastric tissue layers. This suggests that microemulsion-based delivery amplifies both the availability and the functional impact of the plant extract in addressing diabetic complications. The effectiveness at a substantially lower dose compared to conventional extract ranges of 300–450 mg/kg BW hints at improved adherence potential and cost efficiency. Additionally, the system's spontaneous formation and thermodynamic stability support manufacturability without complex infrastructure, strengthening its feasibility as an accessible herbal therapeutic. Nevertheless, extended in vivo safety profiling remains essential, including long-term hepatic, renal, and gastrointestinal evaluations, alongside mechanistic studies, pharmacokinetic mapping in humans, storage stability testing, and economic feasibility comparisons with traditional formulations.

ACKNOWLEDGMENT

Acknowledgment is extended to the Higher Education Service Institution of Region XVI and the Pelita Mas Palu College of Pharmacy for providing infrastructural support. Financial backing was secured for the 2024 fiscal cycle through contract SP DIPA-023.17.1.690523/2024 issued by the Directorate of Research, Technology, and Community Service under the Directorate General of Higher Education, Research, and Technology within the Ministry of Education, Culture, Research, and Technology.

REFERENCES

[1] Diabetes, A. (2015). International diabetes federation. IDF Diabetes Atlas, 7th edn. Brussels, Belgium: International Diabetes Federation, 33(2): 92135-8. https://links.bioscientifica.com/topic/1085/diabetes.

[2] Central Sulawesi Provincial Health Office. (2023). Health Profile of Central Sulawesi Province. Central Sulawesi Provincial Health Office, Palu, Indonesia.

[3] Tandi, J., Mariani, N.M.I., Setiawati, N.P. (2019). Potential of ethanol extract of African leaves (Gymnanthemum Amygdalinum) on decreasing blood glucose levels and pancreatic histopathology of male white rats induced by streptocotocin and high fat feed. Majalah Farmasetika, 4(1): 66-77. https://jurnal.unpad.ac.id/farmasetika/article/view/25861.

[4] Tandi, J., Sutrisna, I., Pratiwi, M., Handayani, T.W. (2020). Potential Test of Nephropathy Sonchus arvensis L. Leaves on Male Rats (Rattus norvegicus) Diabetes Mellitus. Pharmacognosy Journal, 12(5). https://doi.org/10.5530/pj.2020.12.158

[5] Suharti, N., Armenia, A., Abdillah, R., Ramadan, C.M. (2024). Roselle Calyx (Hibiscus Sabdariffa. L) as an anti-diabetic. International Journal of Applied Pharmaceutics, 16(1): 105-110. https://doi.org/10.22159/ijap.2024.v16s1.25

[6] Handayani, T.W., Anggi, V., Afrizal, Magfirah, Tandi, J. (2022). Potential test of soy-yamghurt against antidiabetic in male white rats (rattus norvegicus) streptozotocin induced. Research Journal of Pharmacy and Technology, 15(9): 4139-4143. https://doi.org/10.52711/0974-360X.2022.00695

[7] Ashok, P., Meyyanathan, S.N., Jawahar, N., Vadivelan, R. (2020). Irbesartan formulation and evaluation of

loaded solid lipid nanoparticles by microemulsion techinque. Asian Journal of Pharmacy and Technology, 10(4): 228-230. https://doi.org/10.5958/2231-5713.2020.00038.0

[8] Thaker, V., Tahilani, P. (2022). Formulation and charaterization of antifungal drug microemulsion hydrogel for topical drug delivery. Asian Journal of Pharmacy and Technology, 12(2): 101-108. https://doi.org/10.52711/2231-5713.2022.00017

[9] Soelistijo, S. (2021). Guidelines for the Management and Prevention of Type 2 Diabetes Mellitus in Adults in Indonesia 2021. PB PERKENI. https://pbperkeni.or.id/wp-content/uploads/2021/11/22-10-21-Website-Pedoman-Pengelolaan-dan-Pencegahan-DMT2-Ebook.pdf.

[10] Lokhande, S.S. (2019). Microemulsions as promising delivery systems: A review. Asian Journal of Pharmaceutical Research, 9(2): 90-96. https://doi.org/10.5958/2231-5691.2019.00015.7

[11] Ande, S.N., Sonone, K.B., Bakal, R.L., Ajmire, P.V., Sawarkar, H.S. (2022). Role of surfactant and co-surfactant in microemulsion: A review. Research Journal of Pharmacy and Technology, 15(10): 4829-4834. https://doi.org/10.52711/0974-360X.2022.00811

[12] Chakraborty, T., Gupta, S., Saini, V. (2020). In vivo study of insulin-loaded microemulsion topical gel with aloe vera for the treatment of dermatologic manifestation of diabetes. Research Journal of Pharmacy and Technology, 13(9): 4115-4124. https://doi.org/10.5958/0974-360X.2020.00727.1

[13] Yuniar, S. D. (2020). Effect of ethanolic extract red gedi leaves (Abelmoschus manihot L. Medik) to mikroalbuminuria levels and histopathology of kidney organs in rats with diabetic nephropathy which is induced streptozotocin-nicotinamide. Universitas Setia Budi Repository. https://repo.setiabudi.ac.id/id/eprint/1189/1/INTISARI%20DAN%20ABSTRACK.pdf.

[14] Smeriglio, A., Barreca, D., Bellocco, E., Trombetta, D. (2016). Proanthocyanidins and hydrolysable tannins: Occurrence, dietary intake and pharmacological effects. British Journal of Pharmacology, 174(11): 1244-1262. https://doi.org/10.1111/bph.13630

[15] Tandi, J., Muthi'ah, H.Z., Yuliet, Y., Yusriadi, Y. (2016). Effectiveness of red gedi leaf extract on glucose blood, malondialdehyde, 8-hydroxy-deoxyguanosine, insulin diabetic rats. Journal of Tropical Pharmacy and Chemistry, 3(4): 264-276. https://doi.org/10.30872/j.trop.pharm.chem.v3i4.17

[16] Calabrese, E.J., Mattson, M.P. (2017). How does hormesis impact biology, toxicology, and medicine?. NPJ Aging and Mechanisms of Disease, 3(1): 13. https://doi.org/10.1038/s41514-017-0013-z

[17] Campbell Jr, J.L., Clewell, R.A., Gentry, P.R., Andersen, M.E., Clewell III, H.J. (2012). Physiologically based pharmacokinetic/toxicokinetic modeling. In Computational Toxicology, pp. 439-499. https://doi.org/10.1007/978-1-62703-050-2_18

[18] Aspadiah, V., Wahyuningrum, S.N., Fristiohady, A. (2020). Review article: The use of stearic acid lipids in nanoparticle-based drug delivery systems. Media Farmasi, 21(1): 141-154. https://doi.org/10.32382/mf.v16i2.1622

[19] Talegaonkar, S., Azeem, A., Ahmad, F.J., Khar, R.K., Pathan, S.A., Khan, Z.I. (2008). Microemulsions: A novel approach to enhanced drug delivery. Recent Patents on Drug Delivery & Formulation, 2(3): 238-257. https://doi.org/10.2174/187221108786241679

[20] Lawrence, M.J., Rees, G.D. (2000). Microemulsion-based media as novel drug delivery systems. Advanced Drug Delivery Reviews, 45(1): 89-121. https://doi.org/10.1016/S0169-409X(00)00103-4

[21] Callender, S.P., Mathews, J.A., Kobernyk, K., Wettig, S.D. (2017). Microemulsion utility in pharmaceuticals: Implications for multi-drug delivery. International Journal of Pharmaceutics, 526(1-2): 425-442. https://doi.org/10.1016/j.ijpharm.2017.05.005

[22] Tian, H., Zhang, T., Qin, S., Huang, Z., Zhou, L., Shi, J., Shen, Z. (2022). Enhancing the therapeutic efficacy of nanoparticles for cancer treatment using versatile targeted strategies. Journal of Hematology & Oncology, 15(1): 132. https://doi.org/10.1186/s13045-022-01320-5

[23] Yadav, N., Ganguli, A.K. (2021). Mechanistic understanding of growth of nanorods in microemulsions. Journal of the Indian Chemical Society, 98(3): 100038. https://doi.org/10.1016/j.jics.2021.100038

[24] Jagtap, S.R., Phadtare, D.G., Saudagar, R.B. (2016). Microemulsion: A current review. Research Journal of Pharmaceutical Dosage Forms and Technology, 8(2): 161-170. https://rjpdft.com/HTML_Papers/Research%20Journal%20of%20Pharmaceutical%20Dosage%20Forms%20and%20Technology__PID__2016-8-2-11.html.

[25] Kartsev, V.N., Polikhronidi, N.G., Batov, D.V., Shtykov, S.N., Stepanov, G.V. (2010). A model approach to the thermodynamics of microemulsion systems: Estimation of adequacy of the two-phase model of microemulsions. Russian Journal of Physical Chemistry A, 84(2): 169-175. https://doi.org/10.1134/S0036024410020044

[26] Yuliet, K.K., Widodo, A., Sharon, N., Tandi, J. (2021). Immunostimulant activity of hantap (sterculia coccinea jack) leaves extract on the spesific and non specific immune responses. The 3 Bandung International Teleconference on Pharmacy 2023, 2.

[27] Govindula, A., Reddy, S., Manasa, P. (2019). Phytochemical investigation and in vitro antidiabetic activity of melothria scabra. Asian Journal of Pharmaceutical Research and Development, 7(4): 43-48. https://doi.org/10.22270/ajprd.v7i4.553.

[28] Handayani, D.L., Yusriadi, Y., and Hardani, R. (2017). Microemulsion formulation of purified red spinach leaf extract (Amaranthus Tricolor L.) as an antioxidant supplement. Galenika Journal of Pharmacy, 3(1): 1-9. https://doi.org/10.22487/j24428744.2017.v3.i1.8133

[29] Tandi, J., Handayani, T.W., Widodo, A. (2021). Qualitative and quantitative determination of secondary metabolites and antidiabetic potential of Ocimum Basilicum L. Leaves extract. Rasayan Journal of Chemistry, 14(1): 622-628. https://rasayanjournal.co.in/admin/php/upload/3109_pdf.pdf.

[30] Li, M., Ding, L., Cao, L., Zhang, Z., et al. (2025). Natural products targeting AMPK signaling pathway therapy, diabetes mellitus and its complications. Frontiers in Pharmacology, 16: 1534634.

https://doi.org/10.3389/fphar.2025.1534634
[31] Mekkaoui, A., Li, Y., Ran, Z., Cai, Y., Zhao, L., Xu, B., Wang, C. (2024). Modulation of lipid digestion by nanoarchitectonics of complex interfacial structures with tween 80 and lecithin. Journal of Oleo Science, 73(8): 1125-1134. https://doi.org/10.5650/jos.ess24097
[32] Lu, D., Rhodes, D.G. (2000). Mixed composition films of spans and tween 80 at the air−water interface. Langmuir, 16(21): 8107-8112.
[33] Güçlü-Üstündağ, Ö., Mazza, G. (2007). Saponins: Properties, applications and processing. Critical Reviews in Food Science and Nutrition, 47(3): 231-258. https://doi.org/10.1080/10408390600698197
[34] Putri, W.C.W., Yuliawati, Y., Rahman, H. (2021). Hepatoprotective activity of rambutan leaf (Nephelium Lappaceum L.) ethanol extract in male mice induced by paracetamol. Pharmacon: Indonesian Journal of Pharmacy, 18(2): 148-156. https://repository.unja.ac.id/36170/.
[35] Nahid, S., Mazumder, K., Rahman, Z., Islam, S., Rashid, M.H., Kerr, P.G. (2017). Cardio- and hepato-protective potential of methanolic extract of Syzygium cumini (L.) Skeels seeds: A diabetic rat model study. Asian Pacific Journal of Tropical Biomedicine, 7(2): 126-133. https://doi.org/10.1016/j.apjtb.2016.11.025
[36] Flores-Estrada, J., Cano-Martínez, A., Ibarra-Lara, L., Jiménez, A., Palacios-Reyes, C., García, L.J.P., Ortiz-López, M.G., Rodríguez-Peña, O.N., Hernández-Portilla, L.B. (2025). Spinach extract reduces kidney damage in diabetic rats by impairing the AGEs/RAGE axis. International Journal of Molecular Sciences, 26(10): 4730. https://doi.org/10.3390/ijms26104730
[37] Zhang, L., He, S., Liu, L., Huang, J. (2024). Saponin monomers: Potential candidates for the treatment of type 2 diabetes mellitus and its complications. Phytotherapy Research, 38(7): 3564-3582. https://doi.org/10.1002/ptr.8229
[38] Yuniar, S.D. (2018). The effect of ethanol extract of red gedi leaves (Abelmoschus Manihot L.Medik) on microalbuminuria and kidney histopathology in diabetic rats with streptozotocin-nicotinamide-induced nephropathy. Medicine, Environmental Science. https://www.semanticscholar.org/paper/PENGARUH-EKSTRAK-ETANOL-DAUN-GEDI-MERAH-manihot-DAN-Yuniar/5135508c0adc2e4ef4bccc1803939cb34ac3d171.
[39] Vasylaki, A., Ghosh, P., Jaimes, E.A., Williams, R.M. (2024). Targeting the kidneys at the nanoscale: Nanotechnology in nephrology. Kidney360, 5(4): 618-630. https://doi.org/10.34067/KID.0000000000000400
[40] Elekofehinti, O.O., Oyedokun, V.O., Iwaloye, O., Lawal, A.O., Ejelonu, O.C. (2021). Momordica charantia silver nanoparticles modulate S OCS/JAK/STAT and P13K/Akt/PTEN signalling pathways in the kidney of streptozotocin-induced diabetic rats. Journal of Diabetes & Metabolic Disorders, 20: 245-260. https://doi.org/10.1007/s40200-021-00739-w